ELSEVIER

Ultramicroscopy 67 (1997) 105–111

ultramicroscopy

Lattice imaging using plasmon energy-loss electrons in an energy-filtered transmission electron microscope

Z.L. Wang*

School of Materials Science and Engineering, Georgia Institute of Technology, Atlanta, GA 30332-0245, USA

Received 8 July 1996; revised 30 October 1996; accepted 8 December 1996

Abstract

Lattice images formed by plasmon energy-loss electrons in an energy-filtered transmission electron microscope are compared for different experimental parameters. The image resolution is primarily determined by chromatic aberration which is controlled by the width of the energy selection window. With an energy slit 3 eV in width, the plasmon loss electron image shows the same resolution and contrast as that recorded using the zero-loss electrons in a 300 kV transmission electron microscope equipped with a LaB_6 gun. A discussion on the image resolution in reference to the width of the energy window is given.

PACS: 61.16.-d; 61.14.Rg

Keywords: Lattice imaging; Plasmon; Energy filtering

1. Introduction

Conventional high-resolution transmission electron microscopy (HRTEM) is dominated by phase-contrast, which is the coherent interference property of elastically scattered waves. The HRTEM images are usually recorded without the use of an energy filter, so that both the elastically and inelastically scattered electrons contribute to the image. The inelastically scattered electrons tend to reduce the image contrast due to their incoherence and the effects of chromatic aberration. This makes quantitative data analysis difficult because only the elastic scattering of electrons can be accurately simulated using dynamical theories.

For high-resolution lattice imaging, filtering of inelastically scattered electrons in the recorded image has become technically feasible only in recent years [1–6]. An energy filter can remove all of the inelastically scattered electrons except those scattered by phonons, which typically suffer an energy loss less than 0.1 eV, much less than either the resolution of the filter or the energy spread of

* Corresponding author. E-mail: zhong.wang@mse.gatech.edu.

PII S0304-3991(96)00097-6

the emission source. The energy filter can also be applied to form the images using electrons that have excited a particular crystal state or an inner-shell state of an element in the specimen, forming composition-sensitive images. However, some questions remain regarding the characteristics of the images formed by inelastically scattered electrons. For example, the following questions are of interest: how does inelastic scattering affect the contrast of images formed by elastically scattered electrons and does the image formed by the inelastically scattered electrons have structural features that correspond to the crystallographic structure of the specimen? under what conditions does the contrast observed in the inelastic-electron images preserve the contrast of the elastic-electron image? and what is the achievable resolution in inelastic electron imaging?

This paper is aimed at answering some of these questions. The coherence and incoherence of inelastically scattered electrons are first examined theoretically. Then, lattice images of inelastically scattered electrons are shown as a result of Bragg scattering of the crystal. The experimental parameters that affect the resolution of the inelastic electron image are demonstrated. It is concluded that the images formed by inelastically scattered electrons can offer the same resolution as the elastic electrons if the energy window is smaller than 3 eV. However, the small width of the energy window significantly increases the data acquisition time and noise level.

2. Theory

The original theory for describing the diffraction of inelastically scattered electrons in crystals was given by Kainuma [7] and Yoshioka [8]. In this theory, energy level ε_n and wave vector $\boldsymbol{q}_n$ are the "quantum numbers" used to characterize a crystal state. Electron waves, Ψ_n, inelastically scattered by the same crystal state regardless of the dynamical elastic scattering before and/or after inelastic excitation, are *coherent*. Therefore, the dynamical diffraction of the inelastically scattered electrons, belonging to the same state Ψ_n, has the same characteristics as those of the elastic electrons [9, 10]. It is possible to form lattice images using inelastically scattered electrons, as demonstrated theoretically [11–13] and experimentally [14, 15]. Moreover, electrons inelastically scattered to different excited states Ψ_n and Ψ_m are *incoherent*.

In practice, there are many inelastic states. The experimentally recorded image is an incoherent superposition of the images formed by inelastic electrons belonging to different excited states, provided there is no energy filtering. It is thus generally considered that the inelastic electrons contribute a background. With the energy filtering device, it is now possible to separate the contributions made by the electrons that have undergone different inelastic excitation processes, thus, enabling the fine contrast features in the image to be examined, as shown below.

3. Experimental results

The experiments were performed at 300 kV using an JEOL 3010 high resolution transmission electron microscopy (HRTEM) equipped with a Gatan image filtering (GIF) system that allows acquiring both parallel-detection electron energy loss spectra and energy-selected TEM electron images. The Schertzer resolution of this microscope is 0.17 nm ($C_s = 0.6$ mm and $C_c = 1.3$ mm). A CCD camera, placed at the end of the energy filtering system, allows digital recording of electron images. It must be pointed out that the energy-loss image was recorded with a correction in the kinetic energy of the incident electrons to compensate the chromatic aberration, as incorporated in the design of the GIF system. A detailed description of the experimental method is given elsewhere [6, 16].

3.1. Lattice images formed by inelastically scattered electrons

Using an energy filter, HRTEM lattice images of crystals can be formed with electrons that have suffered energy losses in a well-defined narrow band by inelastic interactions with the crystal. Selecting the width of the energy window is vitally important in forming lattice images, because the intensity distribution of the electrons with energy

losses within the energy window is equivalent to the energy spread of an electron source, which gives serious chromatic aberration. It is known that the contrast in an image recorded from an TEM equipped with a field emission gun (with energy spread 0.3–0.6 eV) is much better than that recorded with a tungsten filament (with energy spread 1.5–3.0 eV), provided the optical configuration is identical. Fig. 1 shows a comparison of lattice images of a thin Al foil recorded using electrons that have suffered the Al plasmon energy loss using two different widths of the energy window. An Al specimen was chosen because of the sharp volume plasmon peak. It is apparent that the image recorded at $\Delta = 3$ eV shows better contrast than that recorded with $\Delta = 6$ eV, as clearly indicated in the line scan profiles shown in Fig. 1c and Fig. 1d. The 0.234 nm lattice fringes are apparently resolved in Fig. 1b but not in Fig. 1a, indicating the dependence of image resolution on the width of the energy window.

The plasmon-loss electron image shown in Fig. 1 is the result of interference between electrons elastically scattered to different Bragg beams both before and after inelastic excitations. In other words, the lattice image formed by inelastically scattered electrons is the result of dynamical diffraction. Coherent interference between these beams and the production of lattice images is possible because electrons inelastically scattered by the same crystal state (and therefore having the same energy loss and momentum transfer) are still coherent.

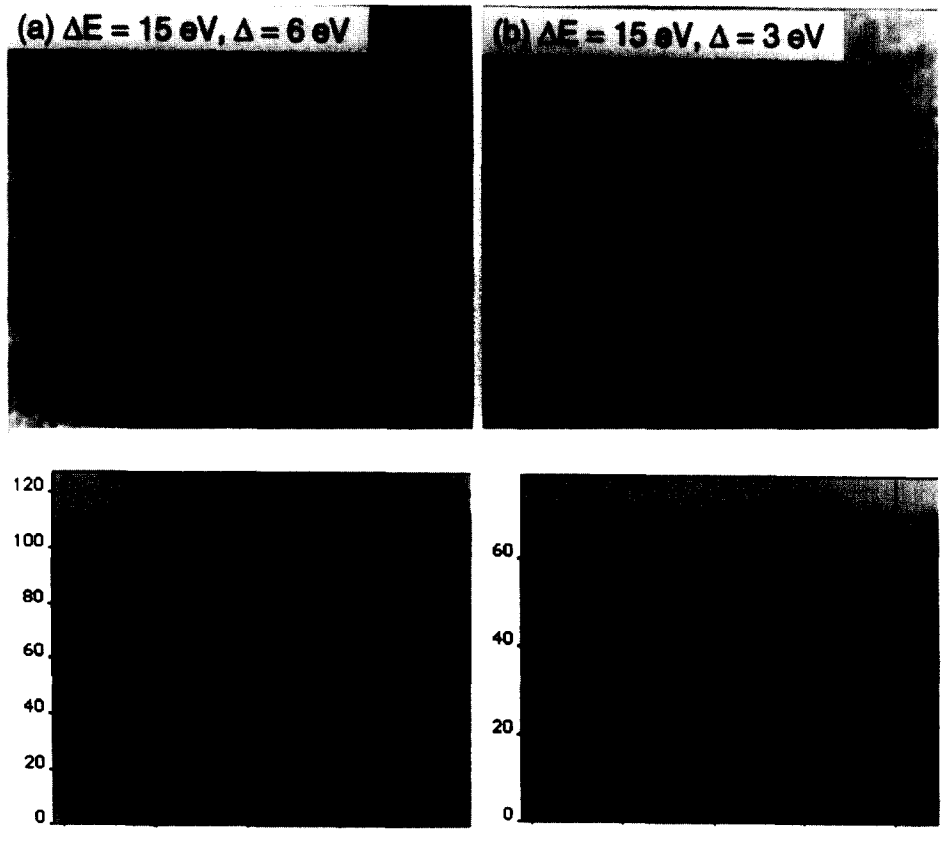

Fig. 1. Plasmon loss energy filtered HRTEM images of Al [1 1 0] recorded using an energy selection slit of width (a) 6 eV and (b) 3 eV, showing the dependence of the image resolution and contrast on chromatic aberration. (c) and (d) are line scan intensity profiles (after averaging for 10 pixels in width) from (a) and (b), respectively, where the distance between the two adjacent peaks is 0.24 nm.

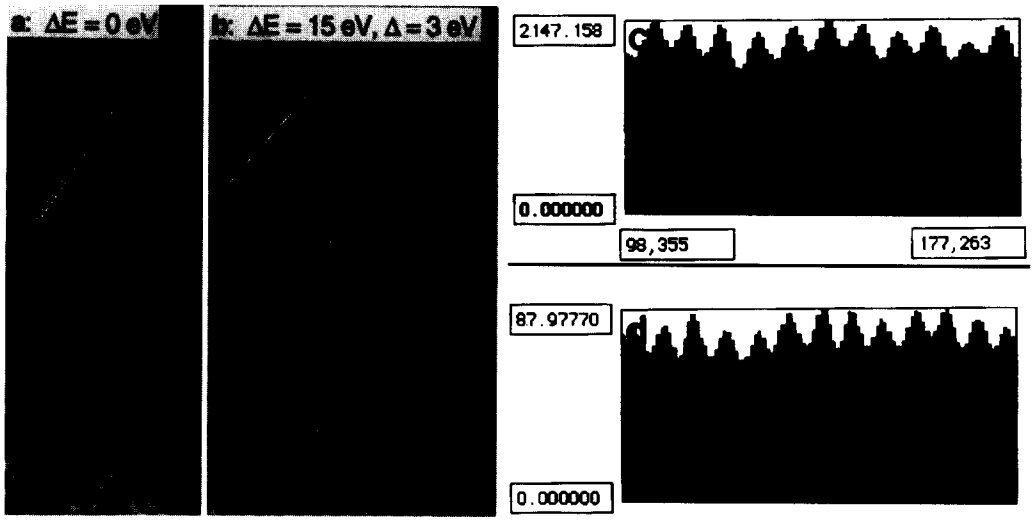

Fig. 2. Energy selected electron images formed by (a) zero-loss and (b) plasmon-loss electrons; (c) and (d) are line scan intensity profiles (after averaging for 10 pixels in width) from (a) and (b), respectively, where the distance between the two adjacent peaks is 0.24 nm.

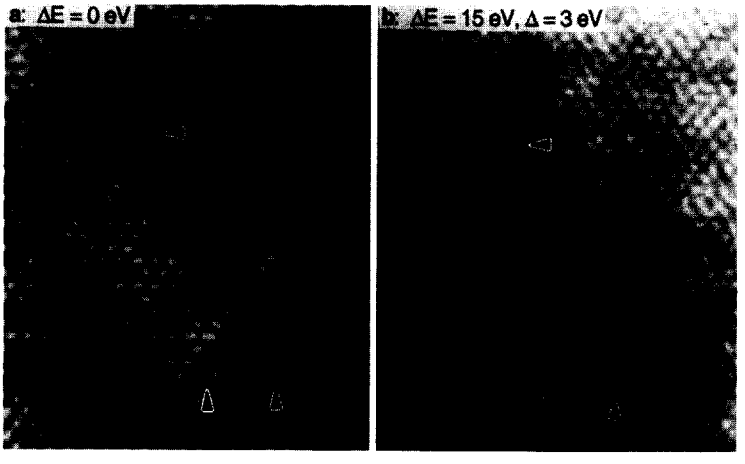

Fig. 3. Energy selected [1 1 0] cross-section HRTEM images of Al/Ti(1 1 1) using (a) zero-loss and (b) 15 eV Al plasmon loss electrons. The width of energy selection slit was 3 eV.

To estimate the optimum image resolution achievable with the inelastic electrons, Fig. 2a and Fig. 2b show a pair of images recorded using the zero-loss and volume plasmon energy-loss electrons, respectively. The photographic images may not give a precise measurement of the image contrast because the contrast is scaled with consideration of the intensities of all the pixels in the image, one dark spot will produce a poor output image contrast. Thus, a line scan is made in each image to precisely examine the contrast and resolution difference, and the results are shown in Fig. 2c and Fig. 2d. No difference in contrast and resolution is visible, but the absolute intensity of the plasmon energy-loss image is much weaker than that of the zero-loss image. Thus, the noise level is the major effect which determines the quality of the plasmon loss image.

Fig. 3 shows lattice images of a cross-section of an Al/Ti (1 1 1) interface recorded when the energy

filter was set to the zero-loss and 15 eV Al plasmon peak, respectively. As divided by the interface along the diagonal direction in the image, the right-hand half is an Al layer, showing strong contrast, while the left-hand half shows less contrast, corresponding to an Ti layer. This contrast difference is due to the selection of the Al plasmon peak for image formation. At the region approaching the interface from the Al side, the image contrast experiences a graduate decrease in intensity. This is because of the localization effect for exciting the Al plasmon loss as a function of the electron impact parameter with respect to the interface, more detailed interpretation was published previously [6]. The visible contrast seen at the Ti side is due to the tail of the Ti plasmon (at 21 eV) falling into the energy-selection window centered at the Al plasmon peak located at 15 eV. After the correction of chromatic aberration, the contrast is preserved between the two images formed by the zero-loss and Al plasmon-loss electrons, and the corresponding points are indicated by arrowheads.

3.2. *Width of energy window and chromatic aberration*

The factors that affect the spatial resolution have been investigated theoretically [17] and experimentally [18, 3], among which the chromatic aberration and signal-to-noise ratio are considered as the major factors. For simplicity, the spherical aberration is ignored in following analysis for the cases with relatively lower image resolution. If the width of the energy window is Δ, the focus spread introduced is

$$f_c = C_c \frac{\Delta}{E_0}, \tag{1}$$

where C_c is the chromatic aberration coefficient of the objective lens and E is the energy of the incident beam. It is known that, in conventional HRTEM phase-contrast imaging under the weak phase approximation, a focus spread introduces an envelope function [19], which limits the transfer of high spatial frequencies by the optical system and is equivalent to introduce a virtual objective aperture. The angular width of the objective aperture in reciprocal space is approximately

$$u_0 \approx \frac{1}{(\pi f_c \lambda)^{1/2}}, \tag{2}$$

The achievable spatial resolution is

$$R \approx (\pi C_c \lambda)^{1/2} \left[\frac{\Delta}{E_0}\right]^{1/2}. \tag{3}$$

For $C_c = 1$ mm and $E_0 = 300$ keV: $R \approx 0.25$ nm if $\Delta = 3$ eV, $R \approx 0.35$ nm if $\Delta = 6$ eV, corresponding to the resolution achieved for the data in Fig. 1; $R \approx 0.45$ nm if $\Delta = 10$ eV, and $R = 0.63$ nm if $\Delta = 20$ eV. Therefore, it is possible to resolve crystal lattices if the width of energy window is less than 3 eV, in agreement with the observation shown in Fig. 1. It must be pointed out, however, that the result given by Eq. (3) applies only to low energy-loss electrons, which are usually referred as delocalized scattering. For a localized scattering process such as the ionization edges, a different approach may be needed.

On the other hand, the signal-to-noise ratio increases if the width of the energy window is decreased. The increase in data acquisition time can also improve the signal-to-noise ratio, but the specimen drift becomes a problem, particularly at high magnification. Moreover, the near edge fine structure introduced by solid state effect strongly affects the signal intensity, thus, the image may not be a precise representation of elemental map because the width of the energy integration above the threshold energy of the ionization edge needs to be larger than 20–50 eV depending on edge type to ensure the proportionality of the acquired signal to the thickness-projected element concentration [16], but the spatial resolution decreases to 1 nm in this case.

It must be pointed out that the chromatic aberration does not affect the spatial resolution of compositional imaging in scanning transmission electron microscopy (STEM) but does affect that in TEM, because the condenser lenses in STEM are placed before the electrons interact with the specimen and there is no lens (with appreciable aberration) between the specimen and the detector. Theoretical calculations have shown that the main effect of low energy-loss electrons (with energy-losses 5–30 eV) is to introduce a focus shift in the lens transfer function due to chromatic aberration

[20]. The image contrast of valence-loss electrons is the same as that of the elastically scattered electrons in STEM but not in TEM. Therefore, the resolution of energy filtered STEM image is mainly determined by the size of the electron probe and the signal-to-noise ratio. In TEM, the image resolution is also affected by the width of the energy-window used to select the inelastic signals, as illustrated above. Therefore, caution must be exercised for using STEM results/theory [21, 22] for interpretation of TEM images.

3.3. Imaging surface steps using inelastic electrons in REM

In reflection high-energy electron diffraction (RHEED), more than 50% of the electrons, in general, suffer energy loss due to the long path-length interaction between the incident electrons and the crystal as well as the crystal surface at grazing-angle reflection geometry [23]. The contrast of the reflected electrons is significantly reduced without energy filtering. This experiment was performed for the GaAs(1 1 0) surface, as described below.

Fig. 4a and Fig. 4b show reflection electron microscopy (REM) images of GaAs(1 1 0) recorded without energy filtering and with zero-loss energy filtering, respectively. The zero-loss filtered (or elastically scattered) electron image shows significantly better contrast and resolution [26]. This is because the inelastically scattered electrons suffer strong chromatic aberration and so produce an out-of-focus background in the image, which is removed

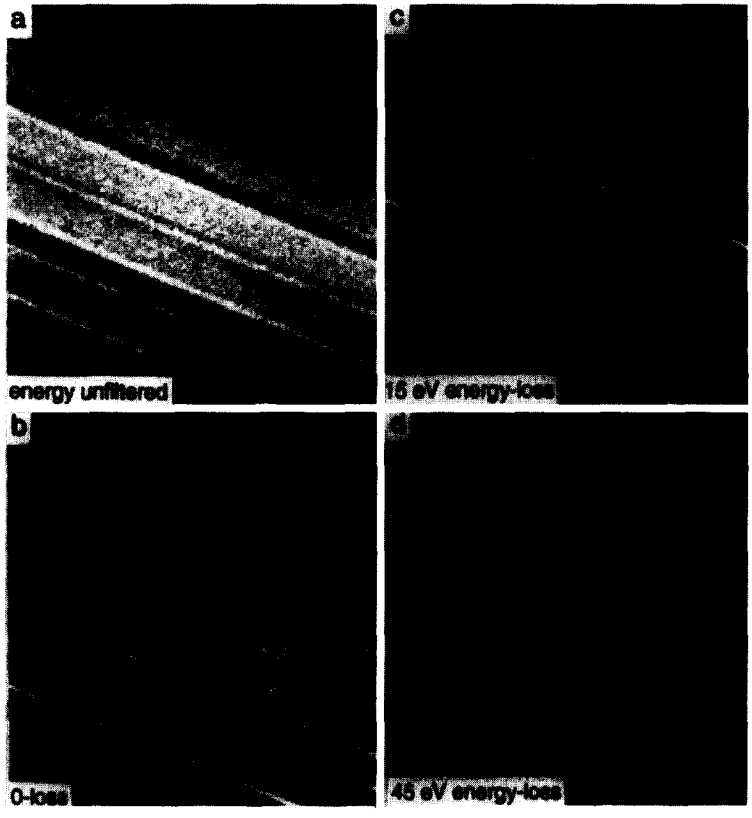

Fig. 4. REM images of GaAs(1 1 0) surface recorded (a) without energy filtering (i.e. the entire electrons), (b) zero-loss energy filtered (i.e., elastic electron), (c) 15 eV energy loss filtered and (d) 45 eV energy loss filtered electrons. Primary beam energy was 300 keV, and energy-selecting window width 10 eV.

by the filter. The fine Fresnel fringes not seen in the unfiltered image are resolved in the zero-loss filtered image. The contrast of the 15 eV energy-loss-filtered image (Fig. 4c) shows better contrast in comparison to the energy-unfiltered image (Fig. 4a), although it is slightly poorer than the image recorded using zero-loss filtered electrons. The contrast in the image recorded using 45 eV energy loss electrons is rather poor owing to multiple inelastic scattering. But the atom-high surface steps are still visible. Since the contrast of atomic steps in REM is dominated by phase-contrast [24], this observation clearly shows that almost the same contrast will be observed if the image is formed using either the elastically or the inelastically scattered electrons.

Since REM images are recorded with a small size objective aperture, the image resolution is determined not only by the beam energy spread and the beam convergence [25] but also largely by the chromatic aberration as introduced by the energy spread of the reflected electrons because of multiple inelastic excitation. With the use of an energy filter, the chromatic aberration effect can be minimized, resulting in an improvement of the image resolution in REM. Therefore, an energy filtering devise is essential for improving the resolution and contrast of REM.

4. Conclusions

In this paper, lattice images formed by Bragg scattering of inelastically scattered electrons are demonstrated. The fringes correspond to the lattice image of the crystal responsible for the Bragg scattering, modulated by an image of the inelastic process. Experimental results showed that the resolution in the images recorded using plasmon energy-loss electrons is primarily determined by the width of the energy selection window. With a 3 eV energy slit, the image obtained using the plasmon loss electrons gives the same contrast and resolution as that formed by the zero-loss electrons. On the other hand, the decrease in the width of the energy window is restricted by the signal-to-noise ratio and the data recording time (or specimen drift).

Acknowledgements

The use of the energy filtering system at the National Institute of Standards and Technology is gratefully acknowledged.

References

[1] L. Reimer, I. Fromm and I. Naundorf, Ultramicroscopy 32 (1990) 80.
[2] J. Mayer, C. Deininger and L. Reimer, in: Energy-Filtering Transmission Electron Microscopy, Ed. L. Reimer, Springer Series in Optical Sciences, vol. 71 (Springer, Berlin, 1995) p.291.
[3] A. Berger, J. Mayer and H. Kohl, Ultramicroscopy 55 (1994) 101.
[4] H. Shuman, C.F. Chang and A.P. Somlyo, Ultramicroscopy 19 (1986) 121.
[5] O.L. Krivanek, A.J. Gubbens and N. Dellby, Microsc. Microstruct. Microanal. 2 (1991) 315.
[6] Z.L. Wang and A.J. Shapiro, Ultramicroscopy 60 (1995) 115.
[7] Y. Kainuma, Acta Crystallogr. 8 (1955) 247.
[8] H. Yoshioka, J. Phys. Soc. Japan 12 (1957) 618.
[9] Z.L. Wang, Elastic and Inelastic Scattering in Electron Diffraction and Imaging (Plenum Press, New York, 1995).
[10] C. Fanidis, D. Van Dyck and J. Van Landuyt, Ultramicroscopy 41 (1992) 55.
[11] A. Howie, Proc. Roy. Soc. A 271 (1963) 268.
[12] A. Howie, J. Microsc. 117 (1979) 11.
[13] C.J. Humphreys and M.J. Whelan, Phil. Mag. 20 (1969) 165.
[14] A.J. Craven and C. Colliex, J. Microsc. Spectrosc. Elect. 1 (1977) 511.
[15] H. Endoh, H. Hashimoto and Y. Makita, Ultramicroscopy 56 (1994) 108.
[16] Z.L. Wang, Microsc. Res. Technique 33 (1995) 279.
[17] A. Berger and H. Kohl, Optik 92 (1993) 175.
[18] O.L. Krivanek, M.K. Kundmann and K. Kimoto, J. Microsc. 180 (1995) 277.
[19] O.L. Krivanek, in: High Resolution Transmission Electron Microscopy and Associated Techniques, Eds. P. Buseck, J. Cowley and L. Eyring (Oxford University Press, New York, 1988) p. 519.
[20] Z.L. Wang and J. Bentley, Microsc. Microstruct. Microanal. 2 (1992) 569.
[21] C. Colliex, Ultramicroscopy 18 (1985) 131.
[22] C. Mory, H. Kohl, M. Tencé and C. Colliex, Ultramicroscopy 37 (1991) 191.
[23] Z.L. Wang, Reflection Electron Microscopy and Spectroscopy for Surface Analysis (Cambridge University Press, Cambridge, 1995), Ch. 11.
[24] J.M. Cowley and L.M. Peng, Ultramicroscopy 16 (1985) 59.
[25] A. Howie, M.Y. Lanzerotti and Z.L. Wang, Microsc. Microstruct. Microanal. 3 (1992) 233.
[26] J.C.H. Spence, in: Energy-Filtering Transmission Electron Microscopy, Ed. L. Reimer, Springer Series in Optical Sciences, Vol. 71 (Springer, Berlin, 1995) p. 401